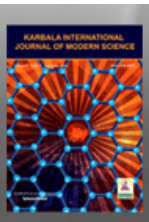

Karbala International Journal of Modern Science

Volume 7 | Issue 4 Article 16

Efficiency of +IDonBlender Photogrammetric Tool in Facial Prosthetics Rehabilitation – An Evaluation Study

Mohammed R. Falih
College of Engineering, University of Baghdad, Baghdad, Iraq, mohammed.r@coeng.uobaghdad.edu.iq

Fanar M. Abed
College of Engineering, University of Baghdad, Baghdad, Iraq, and Honorary member of the University of Exeter, Exeter, UK

Rodrigo Salazar-Gamarra
Plus Identity Institute (+ID) and Paulista University Postgraduate program (UNIP), São Paulo, Brazil

Luciano Lauria Dib
Plus Identity Institute (+ID) and Paulista University Postgraduate program (UNIP), São Paulo, Brazil

Efficiency of +IDonBlender Photogrammetric Tool in Facial Prosthetics Rehabilitation – An Evaluation Study

Abstract

Several open-source 3D modeling software tools have recently been featured to reconstruct a 3D image-based model using Structure from Motion (SfM) algorithms such as +IDonBlender. It is, therefore, necessary to evaluate the accuracy of the models extracted from this tool to prove effectiveness for different applications. This paper aims to evaluate the +IDonBlender methodology tool in rehabilitating facial deformations. +IDonBlender is an add-on tool programmed within Blender software and designed for medical applications. In this research, two individuals from different genders have volunteered to contribute to this study, one with severe facial deformation and the other is healthy with no defects. To assess the robustness of the derived digital model from the +IDonBlender methodology, Agisoft Metashape was used to process the data and create a reference model for comparison purposes. Various scenarios were followed for evaluation: (i) scaling the model based on reference ground truth points, (ii) scaling the model based on known real distance between two reference points, and (iii) cloud-to-mesh (C2M) analysis was applied to individual scenarios to assess the accuracy of the +IDonBlender model through cloud compare analysis. Next, the density analysis of the model was also used to investigate the model resolution for further post-processing and prototyping. The results show that the variation between the tested and the reference models in terms of coordinates and distance measurements was (0.470 mm) and (0.471mm), respectively. Despite the fact that the +IDonBlender model resolution was lower than the Metashape model, the overall results delivered acceptable geometric error values. Therefore, following visual and statistical point clouds data analysis, one can claim the robustness of the +IDonBlender 3D modeling tool for maxillofacial rehabilitation, surgical planning and other clinical applications.

Keywords

Medical SfM-MVS Photogrammetry, Blender, Facial Prosthetics, Rehabilitation Assessment, Geometric Evaluation

Cover Page Footnote

The authors wish to express their thanks to the department of surveying engineering at the University of Baghdad for their help, the individuals who have volunteered to be part of the case study and Hayder Al-Mirza at the department of civil engineering for his contribution regarding the grammatical corrections.

1. Introduction

Patients who may experience cancer treatments, accidents, or congenital diseases can suffer from facial defects [1,2]. As part of the solution, 3D digital workflow procedures have been increasingly proposed to improve the quality of life under scientific cooperation among medical, engineering, artistic, and computer-vision fields [3,4]. For medical applications, body anatomy scanning requires a high level of accuracy and reliability in the methods used for 3D data acquisition and extraction [5]. Today, the acquisition of 3D body measurements by computer vision and image-based remote sensing techniques is becoming highly essential in clinical studies. 3D modeling methods of the diagnosed human body limb are highly versatile, accessible, and can be used in a variety of medically relevant domains (e.g., replacement of anatomical parts with prostheses, replication of skeletal remains, and so on) [6−8]. Thus, accurate 3D models of human anatomy are needed in clinical routines like diagnosis, computer-assisted surgical operations, follow-up, and other biomechanical applications. There are many techniques used for 3D modeling, including computed tomography (CT), magnetic resonance imaging (MRI), laser scanning, and 3D photogrammetry systems [9,10]. Each technique has weaknesses and strengths, whether in terms of cost or accuracy of the final model. Close-range photogrammetry (CRP) can play a significant role in obtaining an image-based dataset of the damaged 3D body and reconstructing the 3D realistic anatomy with computer-based technologies, reverse engineering (RE) algorithms, and rapid prototyping (RP) [11]. Various software (commercial and open source) can be used for processing the captured images to reconstruct the final model. Commercial software has more functionalities than open source software. On the other hand, the open source software allows professionals to develop their own reconstruction algorithms [12]. Recently, "Blender", which is an open source software, is being used as one of the photogrammetry processing software through the OrtogOnBlender add-on tool along with +IDonBlender methodology. Blender is an open-source 3D reconstruction suite that offers a wide variety of key features, including modeling, rendering, animation, and video editing [13]. The + IDonBlender is a specialized add-on in OrtogOnBlender for designing and manufacturing 3D facial prostheses and related virtual surgery planning. It was developed by the "+ID Institute" as a part of the OrtogOnBlender add-on (OOB), coded inside Blender [3]. This methodology is based on SfM algorithms in reconstructing image-based models like other available open source photogrammetric software. But the efficiency of the final results in this type of software remains different from one application to another and must be evaluated for the required purpose. +IDonBlender has many photogrammetric algorithms for reconstructing the modeling, such as (OpenMVG + OpenMVS (standard), SMVS + MeshLab, Meshroom, and Open MVS Linux on Win). In the past, many studies worked on using 3D photogrammetry in maxillofacial rehabilitation without considering the evaluation of the model. Since 3D facial scanning represents an important tool for taking a digital impression of patients' faces in advanced methods used for maxillofacial rehabilitation in +IDonBlender. Therefore, verifying the accuracy and reliability of the scanning process and the reconstructed models is a prerequisite for clinical applications. Therefore, this study was presented to evaluate the accuracy of the 3D model generated through the +IDonBlender methodology tool in rehabilitating facial deformations. Whereas the +IDonBlender is an add-on tool programmed within the open source Blender software and particularly designed for medical applications, the research focuses on evaluating the generated model through the use of +IDonBlender tool by calculating the error in model point coordinates, linear distances, and surfaces' deviation. It also assesses the resolution of the generated model by taking density analysis into consideration, which highly affects the quality of the printed prototype prosthetics later on. Thus, the contribution of this research as an end result can be summarized as follows:

- Design the optimal data capture plan to deliver the best raw images for facial rehabilitation and prosthetic prototyping through CRP 3D modeling techniques.
- Using reference ground truth points to calculate the global error in the generated 3D model through the +IDonBlender tool.
- Evaluating the +IDonBlender methodology as a free tool in open source software which represents an alternative solution to SfM-MVS commercial photogrammetry software and a practical solution for low-budget clinics.

https://doi.org/10.33640/2405-609X.3167

2. Related works

In the last decades, various low-cost and free photogrammetric software have been invested which depend on SfM algorithm in reconstructing the objects for medical rehabilitation and facial prosthetics. Reference [14] employed photogrammetry to obtain a 3D model to digitally scan the face to be used later to fabricate prostheses for the defective body part by using open-source software and a low-cost device (smartphone). They concluded that this technique could help rehabilitate maxillofacial deformities and represent a practical alternative for low-budget clinics. Later, reference [15] examined the efficacy of digital hand-held cameras to design an orbital prosthesis. Images were shot at a distance of 1.5 m away from the patient with three different levels. The images were processed using free 3D reconstruction software apps (Autodesk 123D Catch, Autodesk, Inc.) and used Z-brush software (Pixologic Inc., USA) for restoring an affected eye. They found that this procedure provides acceptable results and minimizes the cost of data collection and modeling efficiently. However, it is necessary to analyze and compare the results provided by open source software with commercial photogrammetry software to investigate their efficiency for use in medical applications.

Many studies like [16–20] worked on evaluating the facial scanning system in maxillofacial rehabilitation. Reference [16] worked on evaluating two facial scanning systems (structured light (3D CaMega, BWHX), and stereophotogrammetry (3dMD)). For evaluation purposes, ten healthy volunteers (5 males and 5 females) have been selected. They relied on measuring the error in the linear distances in their assessment. Where 21 linear distances were measured for individual volunteers using a Vernier caliper with 0.01 mm accuracy. The authors mentioned that both systems have achieved high reliability and can be used to scan human faces. In a similar study, reference [17] assessed three 3D-scanning systems (Avanto MRI, M4D Scan, and Structure Sensor). The 3dMDface System has been used as a reference for this evaluation. Eight volunteers' faces have been scanned with the three scanning systems. They evaluated the model accuracy as a data percentage (within a 2 mm range from the reference scanning system) and calculated the root-mean-square error (RMSE) in model deviation distance and facial distance surfaces. The results show that M4D Scan achieved the highest accuracy (90% within 2 mm, and the RMSE was 0.71 ± 0.28 mm). The Avanto MRI system delivered (86%, RMSE 1.33 ± 0.46). Whereas the precision of the M4D Scan and Structure Sensor was (0.50 mm ± 0.04 mm) and (0.51 mm ± 0.03 mm), respectively. On the other hand, a study was carried out to evaluate the portable Vectra H1 facial scanning system, and 3dMD was used as a reference [18]. 26 volunteers' faces have been scanned with both systems to obtain results. They considered many aspects for this evaluation (error in linear distances, 3D facial surface deviation, and global RMSE). The authors found that the error value in the outcome measurements was 0.84 mm within (0.19−1.54) mm range distance. However, the average RMSE of the 26 surface-to-surface deviations was 0.43 mm within the (0.33−0.59) mm range. Therefore, they claimed that the Vectra H1 system is appropriate for many clinical applications. In the same context, reference [19] investigated the measurement accuracy of soft tissues obtained from two scanning systems, 3D photogrammetry and Cone Beam Computed Tomography (CBCT). 60 wax facial models have been scanned using the two systems. For validation purposes, they selected 19 linear distances and used a coordinate-measuring machine (CMM) to record the coordinates of the reference points, and a T-test has been applied to compare and analyze the results. It was found that the accuracy of 3D photogrammetry was greater than that of the CBCT for patients with facial deformities taking into consideration the protuberant face areas. However, this accuracy can be highly influenced by the facial deformity area. Furthermore, reference [20] assessed two free facial scanning systems (Bellus3D and +ID ReCap Photo). The (ATOS Core) 3D scanner has been used as a reference to scan a mannequin head and create control points in a local coordinate system for validation purposes. They used (GOM Inspect) software to evaluate the 3D data measurements and found that the accuracy of Bellus3D and +ID ReCap were 0.34 ± 0.14 mm and 0.28 ± 0.06 mm, respectively. Following these acceptable clinical results for both scanning systems, they recommended to use them in planning esthetic restorations.

On the other hand, many evaluation studies have been applied recently to assess the OrtogOnBlender add-on as a professional tool for medical restoration and rehabilitation. Reference [21] presented a comparison between preoperative simulation and post-operative findings, showing a relevant ability of OOB workflow to reproduce surgical movement reliability (<2 mm error). They conclude that OOB can produce accurate soft tissue planning for orthognathic surgery, but mesh deformation methods still require improvements. Furthermore, reference [22] reported a

combined usage of modifiers to obtain high-resolution 3D face models. Also, modifications of the available protocol have been reported when site-specific anatomy is needed to be acquired in some cases [23]. The previous highlighted studies focused on evaluating the 3D photogrammetry systems and not the entire processing through calculating the error in the distance and the surface-to-surface deviation. They lacked an evaluation of geometric measurements of the point clouds forming the model. In addition, model resolution analysis was not taken into consideration. Therefore, this study will address this gap by evaluating the maxillofacial 3D digital model by calculating the error in the point cloud coordinates, linear distances, and surface deviation. The density analysis was also applied to assess the resolution of the generated model, which highly affects the quality of the printed prototype prosthetics.

3. Structure from motion (SfM) photogrammetry

Structure from Motion (SfM) is a photogrammetric computer-vision technique based on automatic image orientation estimation following computer vision algorithms to allow successful orientation of a complex block of images [24]. It depends on several computer vision algorithms such as Scale-Invariant Feature Transform (SIFT) to detect features, Random Sample Consensus (RANSAC) to refine matching results, and Levenberg–Marquardt to minimize re-projection errors. The photogrammetric process in the computer vision environment also includes 3D point cloud extraction following Multi-View Stereo (MVS) algorithms. Therefore, applying a photogrammetric workflow based on computer vision algorithms is usually called SfM-MVS Photogrammetry. These methods are considered very effective in analyzing, understanding, and manipulating images of different types, such as medical images. In general, the SfM workflow consists of three major phases [25], as illustrated in Fig. 1:

1) Detect features from images (points, lines … etc.) which represent key points to match features between images automatically using the SIFT.
2) Estimate cameras' location (using key points and relative pairs of camera location).
3) Generate 3D structures (sparse point clouds) using features and the estimated camera locations, and after that, MVS matching is used to generate dense point clouds.

4. Methodology

Many aspects have been considered to meet the research objectives. These aspects are explained in detail in the next sub-sections.

4.1. Case study

Two people volunteered to take part in this research:

Case 1: A 60-year-old female who has lost her entire left eye socket due to a cancerous tumor. Fortunately, the patient's right eye is still functional, which was later used to rebuild the missing eye using the RE approach.
Case 2: A 50-year-old male who is one of the employees in the Paulista University UNIP postgraduate program offered to be a case study as part of the scientific cooperation with the University of Baghdad. He is healthy and has no defects, and his involvement was solely to evaluate the +IDonBlender model.

Although case study 1 patient has defects in her left eye which need to be restored by fabricating an orbital prosthesis, the main focus in this study is to assess the +IDonBlender model and check its geometric efficiency in order to be utilized to restore the defected part in future work.

4.2. Camera network design

In order to achieve high-quality and low-cost 3D image-based models, the optimal camera positions must be determined and this is called camera network design in CR-Photogrammetry. Several constraints may affect determining the approximate camera positions. These can be classified into three types: range, visibility, and accessibility [27,28]. Range-related constraints represent the most critical constraints that affect the results of the CR procedure. These include imaging scale, resolution, camera field of view (FOV), depth of field (DOF), number and distribution of points, and workspace [27]. Therefore, in this research, we focus on range constraints in designing a camera network as the accuracy of the final medical photogrammetric products is a primary demand, especially in prosthetics rehabilitation applications.

The pixel size (pixel pitch) and the ground sampling distance (GSD) (i.e. the minimum required resolution) are significant factors when determining the maximum

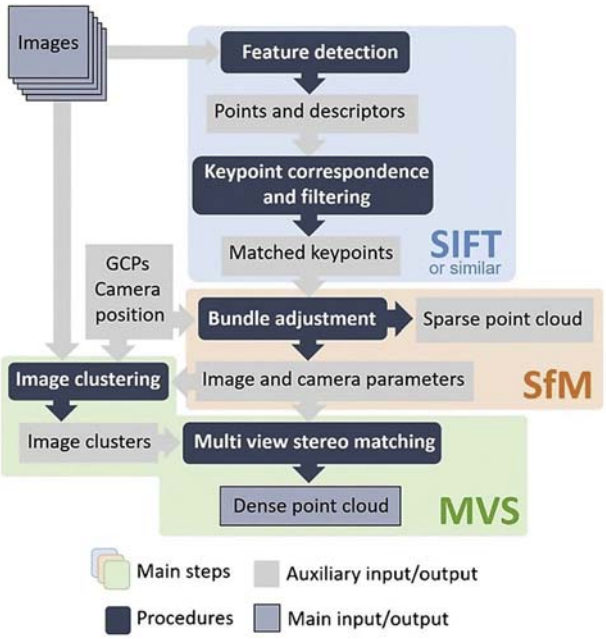

Fig. 1. SfM photogrammetry workflow [26].

range (depth) between the camera and the object [29]. Therefore, in this research, Equation (1) has been applied to determine this range (depth distance) [29]:

$$Depth = GSD*f/pixel \quad (1)$$

where GSD represents the amount of ground coverage per pixel, f is the camera's focal length, and *pixel* is the camera pixel size.

In camera network design, we assumed that the shape of the patient's head is circular, and by using the arc length formula and trigonometry laws, the exposure stations were determined, which is depending on the (i) base to height (B/H) ratio and (ii) images overlap value. In order to compute the relationship between the B/H value and the ground coverage of camera position estimation (G), Equations (2)–(9) were applied and as described below. Fig. 2 shows the image-network design assumptions and Fig. 3 shows the parameters used for image network calculation.

After setting the object distance (H) and the given (B/H) ratio value, it is easy to calculate the distance between two adjacent stations (B). Then, by applying the law of sine, the angle (θ) was calculated, which represents the angle between the two successive camera stations and as shown in Equation (2):

$$\theta = 2*\sin^{-1}(B/2*H) \quad (2)$$

Then the number of capture stations can be easily calculated according to Equation (3):

$$No.of\ station = 360/\theta \quad (3)$$

It is useful to add an additional capture station to ensure full coverage of the object to be photographed. On the other hand, to calculate the overlap between the images, which represents a distance on the circle (arc distance), we must first calculate the central angle corresponding to this arc, which is ($2\varepsilon + \theta$). The angle (α) in Fig. 3 represents half of the angle whose sides are tangential to the object (patient's head). This angle is governed by two main factors: focal length (f) and object distance (H), and to be more specific, it is inversely proportional to (f) and directly proportional to (H) and can be calculated by Equation (4).

$$\alpha = \sin^{-1}(r_{obj.}/H) \quad (4)$$

where $r_{obj.}$ represents the radius of the object, and H represents the object distance.

Then after (ϵ) can be calculated as follows:

$$\varepsilon = 90^{\circ} - \alpha - \theta \quad (5)$$

Now, after calculating the central angles, it is easy to calculate the amount of coverage by applying the arc length formula and as follows:

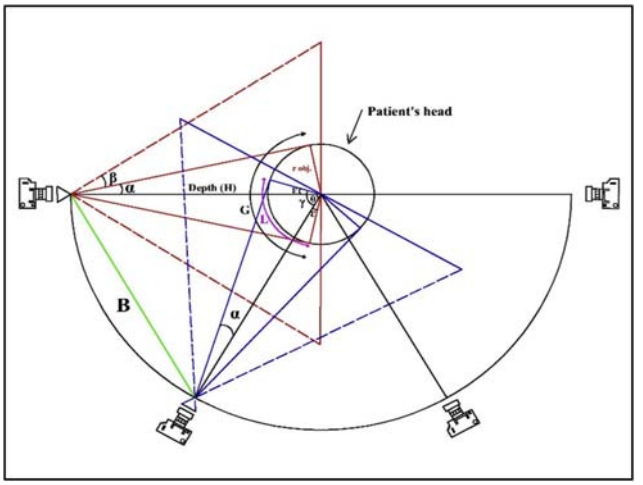

Fig. 2. Image-network design assumptions.

$$L = (2\epsilon + \theta)^{\circ}\pi r_{obj.}/180^{\circ} \quad (6)$$

where $(2\epsilon+\theta)^{\circ}$ represents the central angle (in degrees), and $r_{obj.}$ is the object radius.

However, to show how the endlap value of the adjacent overlapping images can be used to estimate the base distance between adjacent camera stations (B), the following formulas are adopted following the same assumption illustrated in Figure (2). To estimate (B), we need to calculate the amount of (θ) angle as shown in Equations (7) and (8).

$$\theta = 2\gamma - (L^{*}180/r_{obj.}) \quad (7)$$

$$L = 2\gamma\pi r_{obj.}{*}Endlap/180 \quad (8)$$

where γ represents the co-angle of half of the angle whose sides are tangential to the object $(90 - \alpha)$. L is the coverage value, and $r_{obj.}$ is the radius of the object.

Then by applying the sine law, B can be simply estimated according to Equation (9):

$$B = 2{*}H{*}\sin(\theta/2) \quad (9)$$

Now, when the distance between adjacent stations (B) is known as the angular value, which is denoted by (θ) in the above formulas, the number of exposure stations can be easily estimated by applying Equation (3). Moreover, all the above equations were translated into an interactive interface file using a Microsoft Excel sheet to facilitate the calculation process for the case study applied in this research or any other case.

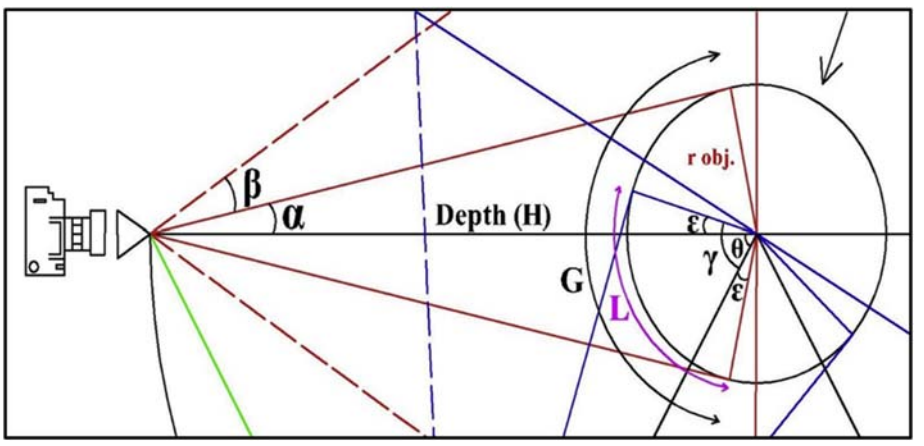

Fig. 3. The illustration of the parameters used for image network calculation.

4.3. Image quality and coded targets design

Following the recommendations from SfM applications literature, it was necessary to deliver the optimal image quality of the AOI from the optimal available camera sensor to reconstruct an accurate 3D model of the facial prosthetics. Therefore, in this research, a simple test was carried out using three different camera sensors (iPhone 11 Pro Max, Nikon D7500, and Nikon D5200) to discover which of these sensors can provide the highest quality and sharpest images for post-processing. Images were taken for a specific scene from three different positions and four images with different height levels are captured for each individual position. Agisoft Metashape software was used for calculating the image quality through the "*Estimate Image Quality*" tool. Table 1 shows the recorded results. It was found that the best image quality could be delivered from the iPhone 11 Pro Max despite using the same camera settings for all sensors. It is also recommended to capture the images in raw format to keep the original quality of the camera sensor as is. However, most SfM-MVS photogrammetric software, such as Agisoft Metashape, doesn't support all raw image formats. As a result, they must be converted to one of the supported formats by keeping the quality as good as possible through third-party software such as Adobe Lightroom, Photoshop, or others. Meanwhile, for geometric validation purposes and to set the correct scale of the generated facial prosthetics, reference points, known as coded targets, with known coordinates must be placed on specific locations in the scene before the photo session. These targets were designed to be identified and detected automatically by the software to overcome the errors resulting from manual identification during image-processing. These targets can improve the automatic matching process during camera alignment and can also be used as reference points for the coordinate system and scale definition [30]. A reliable and popular method for achieving the optimum target size and position and therefore delivering accurate matching results among multi-view images is to distribute coded targets on the measured object. Therefore, circular coded targets centered on a central circular target surrounded by a coded band are commonly used. When the number of pixels in the coded band is small or the projection angle is high, decoding the target can be difficult [31]. In order to determine the appropriate size of the targets that Metashape software can detect automatically, a simple test was performed. A Nikon D5200 camera with 35 focal length with 0.11 mm GSD was used for capturing photos in this test. The distance between the camera station and the plate used to pin the targets was 1 m, and different sizes of targets/center point diameter (from 1 mm to 12 mm) were placed on the plate. Then, three shots were taken for each selected target size, one was vertical and two were tilted at an angle of 25° from the right and left hand sides, as shown in Fig. 4. According to the results shown in Table 2, the 3.2 mm diameter coded target was the smallest size that was completely detected from all angles, which is equivalent to 29 pixels. This equivalent value was calculated by dividing the center point diameter on the GSD value (3.2 mm/0.11 mm = 29 pixels). Thus, the smallest diameter that can be completely detected from all angles when using the iPhone camera sensor is 4.75 mm (29*0.165 = 4.78 mm), and to ensure that all targets will be detected, the 5 mm diameter target was chosen to be used in the patient photo session.

Table 1
Image quality values delivered from different camera sensors.

Capturing Positions	Images	iPhone 11 Pro Max	Nikon D7500	Nikon D5200
Position 1	1	0.912874	0.836932	0.660569
	2	0.965978	0.893284	0.801430
	3	1.009170	0.887010	0.792535
	4	1.021020	0.964321	0.856980
Position 2	1	1.006140	0.620304	0.597350
	2	1.001480	0.714953	0.624827
	3	1.035790	0.622878	0.593727
	4	1.070750	0.494557	0.591870
Position 3	1	1.043420	0.644331	0.581744
	2	1.012310	0.650054	0.632098
	3	1.013570	0.650080	0.576123
	4	0.975726	0.610475	0.586496

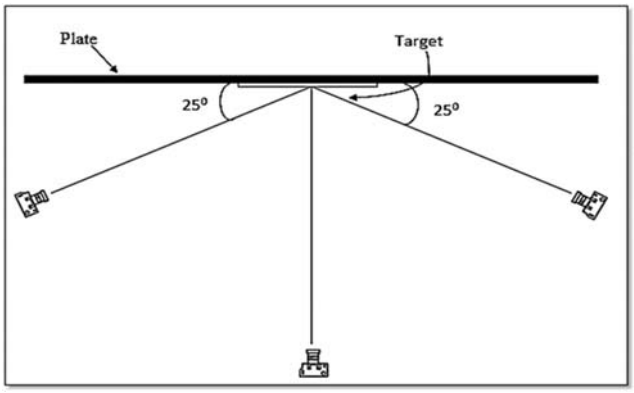

Fig. 4. Imaging scenario used to determine the appropriate size of the coded targets.

4.4. Images acquisition

The iPhone 11 Pro Max camera was used for image acquisition in this research and its specifications are shown in Table 3:

A miniature self-design photographic studio was established inside the photogrammetric laboratory in the Surveying engineering department at the College of Engineering/University of Baghdad using simple and available tools (4 flashlights/projector lights, a white-board, and a chair) as shown in Fig. 5. Lighting conditions have been taken into consideration during the photo session as the light should be exposed consistently on the study area. This allows for avoiding shadows within the area during photo capturing and data acquisition. Also, the camera flash was avoided during image capturing because it may cause blurry images and lead to more noisy point clouds data after image processing. Therefore, it can be said that these conditions enable the user to obtain good quality images without underexposing or overexposing to light.

Pictures were taken for the patient with different height levels for the camera for each camera position, and the capturing scenario was from bottom to top in parallel lines similar to flight direction path lines. Equation (1) was applied to calculate the maximum depth in this case study, depending on the GSD value of (0.1 mm), the pixel size value of (0.000991 mm), and a focal length of (6 mm). Hence, the depth value should be (0.61 m) following these selected parameters. In order to involve all the targets in the background, the depth should be increased to up to 1 m. Hence, GSD will be decreased to 0.165 mm, which is an acceptable value in this study.

Table 2
The percent results of the targets detection using the Agisoft Metashape software.

Centre point diameter (mm)	Angle		
	90° (Normal)	25° (left)	25° (right)
1	0%	0%	0%
2	100%	0%	0%
3	100%	80%	80%
3.2	100%	100%	100%
3.4	100%	100%	100%
4	100%	100%	100%
5	100%	100%	100%
6	100%	100%	100%
7	100%	100%	100%
8	100%	100%	100%
9	100%	100%	100%
10	100%	100%	100%
12	100%	100%	100%

4.5. Image-based modeling

Following image acquisition, the 3D model extraction process of the damaged part of the face starts by uploading the images to the SfM-MVS photogrammetric software. Agisoft Metashape was used to process the data and generate a reference model to assess the quality of the digital model extracted from the +IDonBlender add-on. Agisoft is a commercial licensed photogrammetry software considered by the international community as a gold-standard system. The ground control points are used in this research to build a scaled model and later validate the accuracy of the +IDonBlender model. In + IDonBlender, all the steps involved in model building (feature detection, matching process, calculating camera positions and orientation, generating sparse and dense point clouds, meshing, and texturing) are applied as black box

Table 3
The specification of iPhone 11 Pro Max camera.

Camera resolution (MP)	12
Sensor size (mm)	2.99 * 3.99
Camera Pixel size (μm)	0.991
Image resolution (pixel)	4032 * 3024

procedures. The general workflow in +IDonBlender can be described as follows, see Fig. 6:

1) Add photos: adding photos represents the first step in the model building process. This could be achieved by selecting the photo path and clicking "Accept".
2) Select scanning system: +IDonBlender provides various options to the end user. The "OpenMVG + OpenMVS" option is the default used in the software to provide better texture quality. This option also provides a faster workflow than other available options.
3) D factor and smooth factor values: for face digitizing, +IDonBlender recommends keeping these values as the default at 6 and 16 for D factor and smooth factor, respectively. It is important to note that the D factor is the rate of mesh simplification.
4) Start photogrammetry: selecting this option will start the photogrammetry processing where the model will be generated in a black box directly.
5) Align & scale the model: when the model is generated, it usually has arbitrary dimensions. So, to rescale the model, we must measure a horizontal distance such as the width of the nose, the outer distance between the eyes, or the distance between any reference points in the model.
6) Export model: +IDonBlender offers to export the model with various extensions (i.e. *.stl, *.Obj, *.Ply … etc.).

4.6. Model inspection

In this research, CloudCompare has been selected for the inspection process between the IDonBlender add-on model and the reference (Metashape) model. CloudCompare is an open-source, flexible, and user-friendly software used for 3D point cloud analysis and

Fig. 5. A miniature studio designed for photo session.

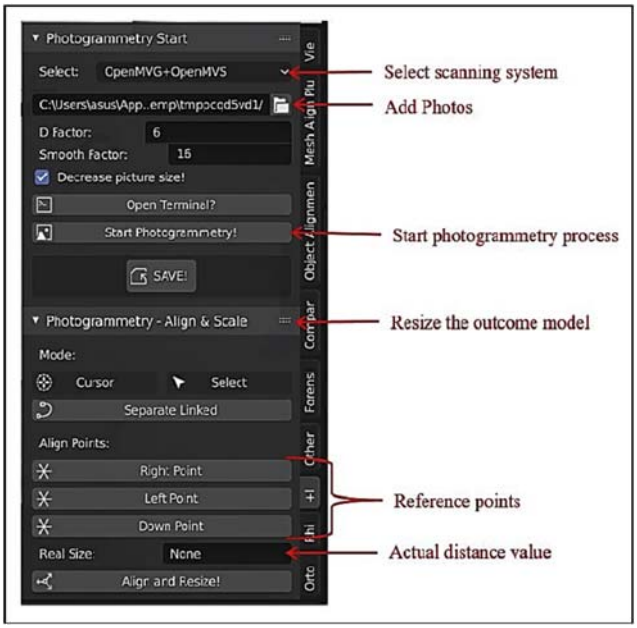

Fig. 6. A typical post-processing workflow in +IDonBlender photogrammetric tool.

3D dataset registration. The + IDonBlender model is inspected with two alignment model scenarios: (i) Align the model in OrtogOnBlender based on a clinical measured distance between two reference points; and (ii) Align the model in CloudCompare based on the selected reference points.

Once the two models are uploaded for inspection, several steps should be followed:

1) Align the IDonBlender model to the reference model by picking at least 4 equivalent points in both models.
2) Register models through minimizing the RMSE differences or increasing the number of iterations.
3) Calculate the cloud-to-cloud or cloud-to-mesh distance.

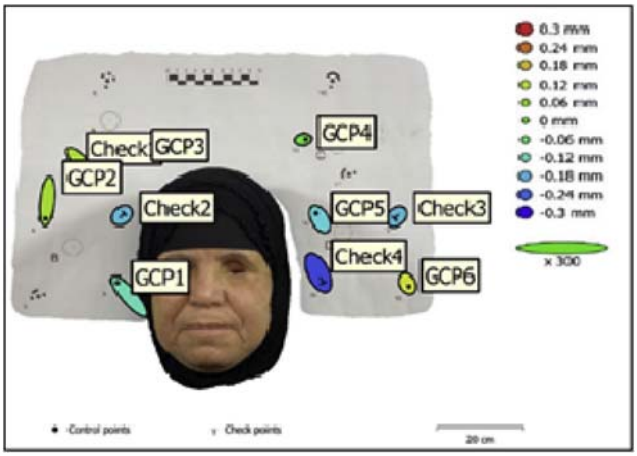

Fig. 7. GCP locations and error estimates.

Table 4
RMSE of control points.

Label	X error (mm)	Y error (mm)	Z error (mm)	Total (mm)	Image (pix)
GCP1	−0.0878882	0.1062960	−0.1241030	0.1855390	0.801 (75)
GCP2	−0.0131461	−0.1355130	0.0961995	0.1667060	1.081 (102)
GCP3	0.0948248	0.0030300	0.0676764	0.1165380	0.964 (100)
GCP4	0.0191826	0.0031570	−0.0264411	0.0328188	1.13 (94)
GCP5	−0.0234876	0.0421476	−0.1557140	0.1630180	0.68 (72)
GCP6	0.0105144	−0.0191176	0.1423820	0.1440440	1.09 (98)
Total	0.0546490	0.0728279	0.1113960	0.1438730	0.990

5. Results and discussions

5.1. Model quality control

The two generated models have been checked based on the coordinates of the reference points as explained:

5.1.1. Metashape model

When uploading photos into the Metashape software, coded targets in source photos are detected automatically through the *Detect Markers* command in the tools menu. The corresponding markers were added to the Reference pane and the coordinates of these reference markers have been uploaded. To validate the Metashape-based model, six reference points have been selected as control points and four points as check points (Fig. 7). Then the software calculated the RMSE for these references and the total errors for control and check points were 0.144 mm and 0.198 mm, respectively (Table 4 & Table 5). After building the model (alignment, building a dense cloud, building the mesh, and texture), the steps have been accomplished, and the model was generated. See Fig. 8.

5.1.2. +IDonBlender model

As mentioned in section 4.5, the model reconstruction process in +IDonBlender has been carried out in a black box procedure. This process includes all the steps needed to create the model, such as: photo alignment, building sparse points, building dense points, generating the mesh, and creating the texture. Fig. 9 illustrates the model obtained after image processing.

5.2. Model inspection

5.2.1. Scaling the model-based on reference points

After creating the model using the +IDonBlender tool methodology, ten reference points have been selected for evaluation (6 control points and 4 check points). Then the model has been scaled in CloudCompare based on these reference points. Following quality assurance analysis, the total error was calculated, with **0.30 mm** and **0.47 mm** for control and check points, respectively. To inspect the model, it was aligned with the reference model based on the reference control points, and the RMSE was **0.30 mm**. The deviation distance between the two models has been computed through the cloud-to-mesh tool. For further analysis, the Gaussian distribution has been applied for cloud-to-mesh distance analysis and the standard deviation was found to be 0.97 mm (before applying the best fitting algorithm) and 0.71 mm (after applying the best fitting algorithm) (see Fig. 10). According to the apparent + IDonBlender model results, it can be noticed that the nose, chin, lower lip, top of the upper lip, and the eye socket have an error of approximately 3 mm. In contrast, the cheek area has an error of approximately 2 mm. Moreover, the rest of the face has an error of (-1− 0.4) mm (see Fig. 11, left). The best fitting algorithm was applied between the two models with RMSE of 0.47 mm in order to make the best

Table 5
RMSE of check reference points.

Label	X error (mm)	Y error (mm)	Z error (mm)	Total (mm)	Image (pix)
Check 1	0.0706439	−0.0791900	0.1034170	0.1481780	0.832 (102)
Check 2	0.0142822	0.0140259	−0.1732450	0.1743980	0.655 (84)
Check 3	−0.0156024	−0.0162463	−0.1732140	0.1746720	0.947 (98)
Check 4	0.0344233	−0.0746689	−0.2596590	0.2723660	0.75 (70)
Total	0.0406907	0.0554688	0.1858320	0.1981570	0.813

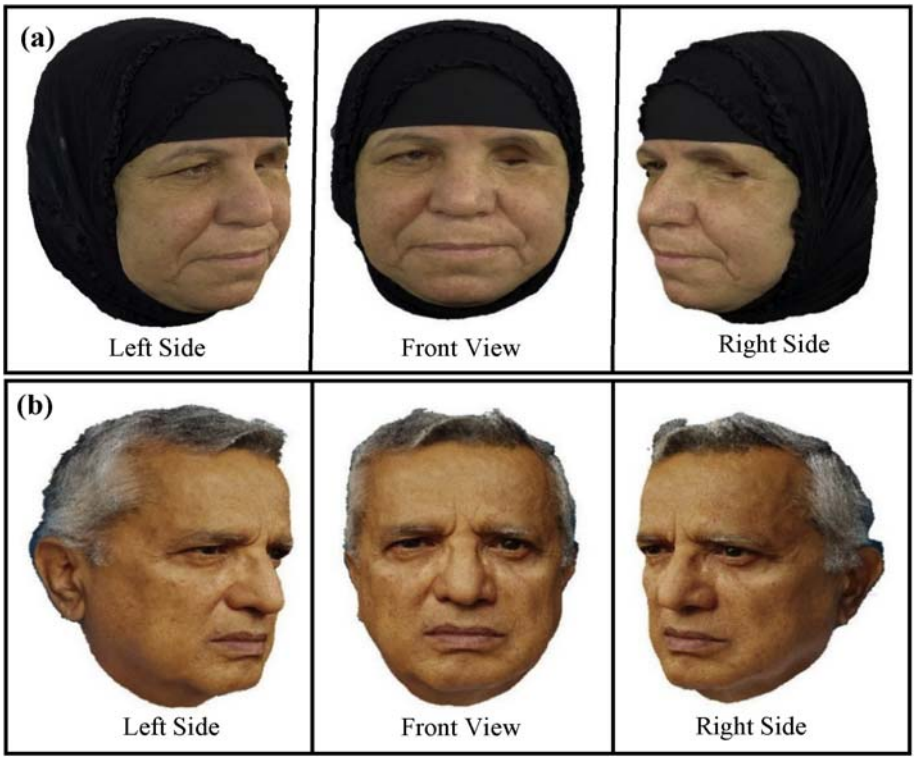

Fig. 8. 3D textured models of two case studies generated with Metashape.

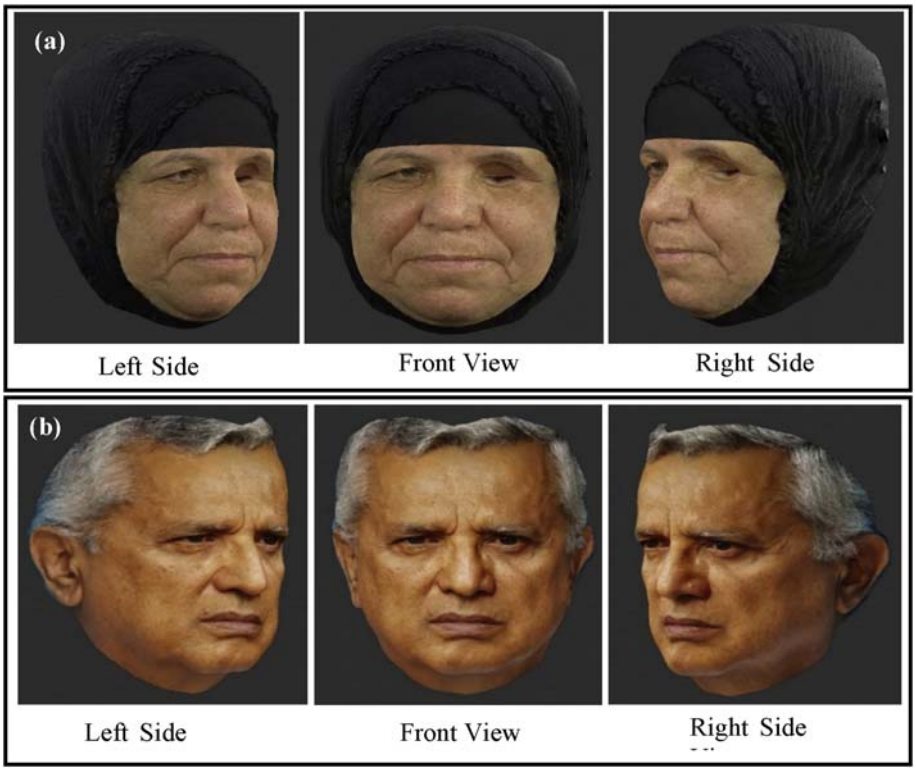

Fig. 9. 3D textured models of two case studies generated with +IDonBlender.

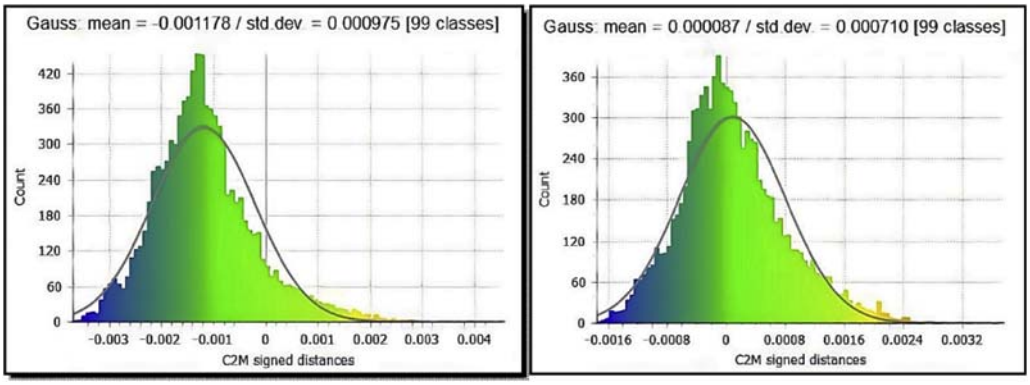

Fig. 10. The Gaussian distribution of the aligned datasets. (Left) Before applying best fitting. (Right) After applying best fitting.

match for validation purposes. The results indicated that the degree of error for the chin and nose areas was reduced to 1 mm, while the error was minimized to 2 mm for the eye socket, and for the rest of the face the error ranged between (−0.5−0.5) mm (see Fig. 11, right).

Although the geometric positioning error in the +IDonBlender model was small, at about 0.47 mm, it was found that there was a deviation in the face area during model construction. This can be clearly seen through the visual inspection (before applying the best fitting algorithm) and the results of the Gaussian distribution analysis where the standard deviation was (0.97 mm) and the mean value was (−1.2 mm). However, when applying the best fitting algorithm to get the best matching with the reference model, we noticed that the mean value was considerably reduced to (0.087 mm) and the standard deviation was also decreased to (0.710 mm).

5.2.2. Scaling the model based on clinical measured distances

As mentioned earlier, the +IDonBlender methodology allows resizing the model to its real dimensions by entering the clinical distance measurements between two reference points built within the model. In this inspection process, the scale bar distance (10 cm) was placed in the background behind the patient's head and used as a clinically measured distance for re-scaling the model. To evaluate the scaled model, various reference distances were selected to be compared with the reference model (see Fig. 12), and the results are shown in Table 6.

According to the results, we found that the process of resizing the model using the known distance gives an acceptable error of (0.471 mm). This error may occur during the model reconstruction process and due to manual distance measurements. As for the second case study, since the photo session took place without

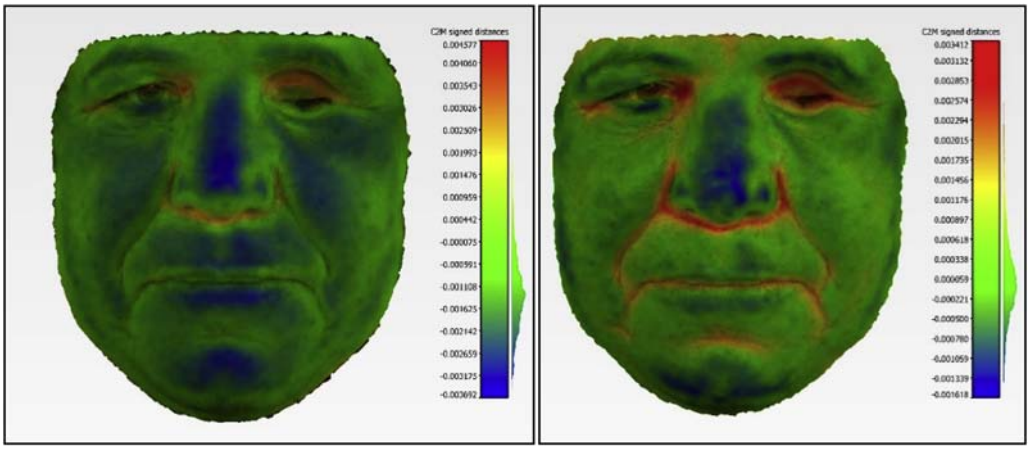

Fig. 11. Visual inspecting of the +IDonBlender model. (Left) Before applying the best fitting algorithm. (Right) After applying the best fitting algorithm.

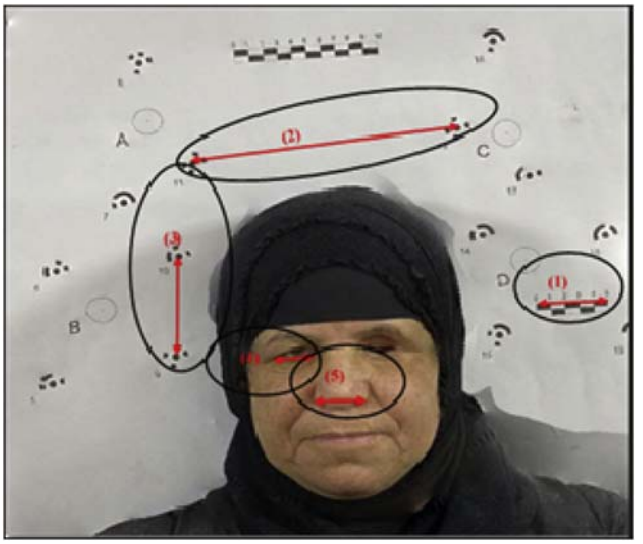

Fig. 12. The selected reference distances used for model evaluation scaling based on clinical measurements.

Table 6
Measured clinical distances and deviations.

Ref. distance	Metashape (m)	+IDonBlender (m)	RMSE (m)
(1) Scale bar (5 cm)	0.050000	0.049487	0.000513
(2) Dist. (11–13)	0.185853	0.185358	0.000495
(3) Dist. (9–10)	0.078706	0.078245	0.000461
(4) Eye length	0.023800	0.023274	0.000526
(5) Nose width	0.038500	0.038142	0.000358
		Total errors	0.000471

placing reference points, it was impossible to build the model using its real dimensions. Therefore, the real distance must be measured between any two points in the model to re-scale it later. As mentioned earlier, to check the generated model, the two inspected and reference models must first be matched using the alignment process, then the best fit algorithm is applied in order to reduce the RMSE value. In this case, 4 points were selected to achieve the alignment process as shown in (Fig. 13, left). As a result, the model has been aligned and registered to the reference model with RMSE of 0.429 mm and 0.327 mm, respectively. Then the difference between the two models was calculated using the cloud-to-mesh tool, (see Fig. 13, right).

Fig. 13. Rescaling case study two. (Left) The distribution of the selected points for alignment. (Right) Visual inspection analysis.

6. Conclusion

In advanced methods of maxillofacial rehabilitation, the accuracy of the digital impression is based mainly on the geometric accuracy of the extracted digital model. Therefore, evaluating the accuracy of the model must be taken into consideration to improve the efficiency of the methodology used for generating the prosthesis of the maxillofacial model. Therefore, this study was performed to evaluate the accuracy of the 3D model generated through the +IDonBlender methodology tool in rehabilitating facial deformations. Where the +IDonBlender is an add-on tool programmed within the open source Blender software and designed particularly for medical applications. The contribution of this study is summarized to designing the optimal data capture plan to deliver the best raw images used in reconstructing the model. The second contribution is evaluating the geometric accuracy of the model extracted through estimating the total error delivered in comparison to ground truth reference measurements. Additionally, this methodology presents the CRP approach as a practical alternative for rehabilitating facial deformations for low-budget clinics. In this evaluation study, several scenarios were used to analyze and examine the model produced using visual and statistical analysis through applying a proposed data capture plan using CRP technique. The total errors in the measured coordinates and distances were calculated and density analysis was applied to assess the resolution of the generated model. Following the results obtained, several conclusions can be delivered:

- +IDonBlender provides an acceptable geometric error for 3D reconstruction of image-based modeling, particularly for the rehabilitation purposes of maxillofacial deformities. This was addressed to be (0.470 mm) relative to the reference truth dataset.
- Resizing the generated model based on real measured distances gives an acceptable error in linear measurements that reaches (0.471 mm).
- Although, the "OpenMVG + OpenMVS" geometric model delivered by + IDonBlender can deliver positive results by achieving acceptable geometric accuracy, there is still a deviation in the correct position of the extracted model. The Gaussian distribution analysis can be used to detect this deviation.
- The best fitting algorithm enables the user to get the best match between the two comparative 3D models as the standard deviation was reduced from (0.975 mm) to (0.710 mm) which led to the normal distribution being close to zero. Also, the mean value was reduced from (1.178 mm) to (0.087 mm).
- Following density analysis application, the resolution achieved from applying the presented methodology and without applying the modifier attribution tool, was low to some extent when compared to the resolution that can be obtained from the reference software.

Following these outcomes, it can be concluded that the +IDonBlender methodology is more effective and geometrically robust for medical applications. Therefore, it is recommended to use the +IDonBlender photogrammetric tool in medical applications such as the rehabilitation of maxillofacial deformities, surgical planning, and a wide range of clinical studies. However, the weaknesses in this evaluation study lie in using a single camera to capture the images and therefore some wide field of view images have been delivered. Therefore, it is recommended to use a multi-camera system to avoid wide field of view images with a faster capturing rate and higher resolution, and thus have a high data acquisition consistency to obtain high quality models. Furthermore, there was a lack in the reference points that were selected for evaluation purposes, as these had been incorrectly targeted at approximately one depth value, which may have affected the total estimated RMSE value. However, it is recommended to address this issue in future studies in order to evaluate the effect of variant depth values on the geometric measurements. For similar approaches, more case studies with complex features are recommended to be considered for validation and accuracy assessment in future studies. It is worth mentioning that additional studies will be carried out and will focus on producing and prototyping a genuine facial case study to determine the feasibility of the presented approach and show its potential for delivering satisfactory results.

Acknowledgement

The authors wish to express their thanks to the department of surveying engineering at the University of Baghdad for their help, the individuals who have volunteered to be part of the case study and Hayder Al-Mirza at the department of civil engineering for his contribution regarding the grammatical corrections.

References

[1] F.M. de Oliveira, R. Salazar-Gamarra, D. Öhman, U. Nannmark, V. Pecorari, L.L. Dib, Quality of life assessment of patients utilizing orbital implant-supported prostheses, Clin Implant Dent Relat Res. 20 (2018) 438−443, https://doi.org/10.1111/cid.12602.

[2] R. Salazar-Gamarra, J. de Oliveira, L. Dib, Aesthetics in maxilofacial rehabilitation, Rev. APCD Estética. 3 (2015) 42−52, https://doi.org/10.13140/RG.2.1.4872.8729.

[3] R. Salazar-Gamarra, C.A.D.C. Moraes, R.M. Seelaus, J.V. Lopes da Silva, J.J. Ulloa, L.L. Dib, Introdução à metodologia "mais identidade": próteses faciais 3d com a utilização de tecnologias acessíveis para pacientes sobreviventes de câncer no rosto, in: A.C. De Oliveira (Ed.), Comun. Científica e Técnica Em Odontol., second ed., ponta Grossa, Brasil, 2019, pp. 251−272, https://doi.org/10.22533/at.ed.265192903.

[4] A. Artopoulos, J.A.N. Buytaert, J.J.J. Dirckx, T.J. Coward, Comparison of the accuracy of digital stereophotogrammetry and projection moiré profilometry for three-dimensional imaging of the face, Int J Oral Maxillofac Surg. 43 (2014) 654−662, https://doi.org/10.1016/j.ijom.2013.10.005.

[5] T.H. Farook, N.B. Jamayet, J.Y. Abdullah, Z.A. Rajion, M.K. Alam, A systematic review of the computerized tools and digital techniques applied to fabricate nasal, auricular, orbital and ocular prostheses for facial defect rehabilitation, J. Stomatol. Oral Maxillofac. Surg. 121 (2020) 268−277, https://doi.org/10.1016/j.jormas.2019.10.003.

[6] M. Javaid, A. Haleem, Additive manufacturing applications in medical cases: a literature based review, Alexandria J. Med. 54 (2018) 411−422, https://doi.org/10.1016/j.ajme.2017.09.003.

[7] D.A. Hussien, F.M. Abed, A.A. Hasan, Stereo photogrammetry vs computed tomography for 3D medical measurements, Karbala Int. J. Mod. Sci. 5 (2019) 202−212, https://doi.org/10.33640/2405-609X.1130.

[8] J. Kaufman, Replication and fabrication of crafted and natural artifacts by reverse engineering using single camera photogrammetry, Doctoral dissertation, Lancaster University, 2018.

[9] R. Struck, S. Cordoni, S. Aliotta, L. Pérez-Pachón, F. Gröning, Application of photogrammetry in biomedical science, in: P.M. Rea (Ed.), Biomed. Vis. Adv. Exp. Med. Biol., Springer, Cham, 2019, pp. 121−130, https://doi.org/10.1007/978-3-030-06070-1_10.

[10] H. Çatal Reis, Detection OF foot bone anomaly USINGMEDICAL photogrammetry, Int. J. Eng. Geosci. 3 (2018) 1−5, https://doi.org/10.26833/ijeg.333686.

[11] G. Sansoni, M. Trebeschi, F. Docchio, State-of-the-art and applications of 3D imaging sensors in industry, cultural heritage, medicine, and criminal investigation, Sensors 9 (2009) 568−601, https://doi.org/10.3390/s90100568.

[12] B. Kloc, A. Mazur, M. Szumiło, Comparison of free and commercial software in the processing of data obtained from non-metric cameras, J. Ecol. Eng. 22 (2021) 213−225, https://doi.org/10.12911/22998993/131074.

[13] Blender 3 Blender, 0 Reference manual, 2021. https://docs.blender.org/manual/en/3.0/. (Accessed 30 May 2021). accessed.

[14] R. Salazar-Gamarra, R. Seelaus, J.V.L. Da Silva, A.M. Da Silva, L.L. Dib, Monoscopic photogrammetry to obtain 3D models by a mobile device: a method for making facial prostheses, J. Otolaryngol. - Head Neck Surg. 45 (2016) 1−13, https://doi.org/10.1186/s40463-016-0145-3.

[15] M. Chiu, S.C. Hong, G. Wilson, Digital fabrication of orbital prosthesis mold using 3D photography and computer-aided design, Graefe's Arch Clin Exp Ophthalmol 255 (2017) 425−426, https://doi.org/10.1007/s00417-016-3544-2.

[16] H. Ye, L. Lv, Y. Liu, Y. Liu, Y. Zhou, Evaluation of the accuracy, reliability, and reproducibility of two different 3D face-scanning systems, Int J Prosthodont 29 (2016) 213−218, https://doi.org/10.11607/ijp.4397.

[17] P.G.M. Knoops, C.A.A. Beaumont, A. Borghi, N. Rodriguez-Florez, R.W.F. Breakey, W. Rodgers, et al., Comparison of three-dimensional scanner systems for craniomaxillofacial imaging, J Plast Reconstr Aesthetic Surg. 70 (2017) 441−449, https://doi.org/10.1016/j.bjps.2016.12.015.

[18] L. Camison, M. Bykowski, W.W. Lee, J.C. Carlson, J. Roosenboom, J.A. Goldstein, et al., Validation of the Vectra H1 portable three-dimensional photogrammetry system for facial imaging, Int J Oral Maxillofac Surg. 47 (2018) 403−410, https://doi.org/10.1016/j.ijom.2017.08.008.

[19] Z. Zhao, L. Xie, D. Cao, I. Izadikhah, P. Gao, Y. Zhao, et al., Accuracy of three-dimensional photogrammetry and cone beam computed tomography based on linear measurements in patients with facial deformities, Dentomaxillofacial Radiol 50 (2021) 20200001, https://doi.org/10.1259/dmfr.20200001.

[20] Y.N.R. Gallardo, R. Salazar-Gamarra, L. Bohner, J.I. De Oliveira, L.L. Dib, N. Sesma, Evaluation of the 3D error of 2 face-scanning systems: an in vitro analysis, Press J. Prosthet. Dent, 2021, pp. 1−7, https://doi.org/10.1016/j.prosdent.2021.06.049.

[21] H.S. Cunha, C.A. da Costa Moraes, R. de Faria Valle Dornelles, E.L.S. da Rosa, Accuracy of three-dimensional virtual simulation of the soft tissues of the face in OrtogOnBlender for correction of class II dentofacial deformities: an uncontrolled experimental case-series study, Oral Maxillofac Surg. 25 (2021) 319−335, https://doi.org/10.1007/s10006-020-00920-0.

[22] R. Salazar Gamarra, C.A.D.C. Moraes, E.L.S. Da Rosa, R. Seelaus, J.V.L. Da Silva, L. Dib, Multiresolution and displacement: modifier attribution to enhance realistic 3D photogrammetry for models of the face, Biomed. J. Sci. Tech. Res. 29 (2020) 22812−22817, https://doi.org/10.26717/BJSTR.2020.29.004864.

[23] C. Moraes, D. Sobral, D.W. Duarte, G.Z. Cavalcanti, R. Salazar-Gamarra, R. Dornelles, Protocolo Complementar para Melhor Resolução do Nariz em Fotogrametria 3D, 2020, https://doi.org/10.6084/m9.figshare.13010300.

[24] E. Dall'Asta, K. Thoeni, M. Santise, G. Forlani, A. Giacomini, R. Roncella, Network design and quality checks in automatic orientation of close-range photogrammetric blocks, Sensors 15 (2015) 7985−8008, https://doi.org/10.3390/s150407985.

[25] O. Özyeşil, V. Voroninski, R. Basri, A. Singer, A survey of structure from motion, Acta Numer 26 (2017) 305−364, https://doi.org/10.1017/S096249291700006X.

[26] J. Iglhaut, C. Cabo, S. Puliti, L. Piermattei, J. O'Connor, J. Rosette, Structure from motion photogrammetry in forestry: a review, Curr. For. Reports. 5 (2019) 155−168, https://doi.org/10.1007/s40725-019-00094-3.

[27] M. Saadatseresht, F. Samadzadegan, A. Azizi, Accessibility analysis in camera placement network design for vision metrology, in: Proc. FIG work. Week, 2004, pp. 1−10. Athens, Greece.

[28] H. Mahami, F. Nasirzadeh, A.H. Ahmadabadian, F. Esmaeili, S. Nahavandi, Imaging network design to improve the automated construction progress monitoring process, Construct Innovat 19 (2019) 386−404, https://doi.org/10.1108/CI-07-2018-0059.

[29] B.S. Alsadik, G. Vosselman, M. Gerke, Guided close range photogrammetry for 3D modelling of cultural heritage sites, Doctoral dissertation, University of Twente, 2014, https://doi.org/10.3990/1.9789036537933.

[30] A.H. Portal, Coded targets and Scale bars, 2020. https://agisoft.freshdesk.com/support/solutions/articles/31000148855-coded-targets-and-scale-bars. (Accessed 10 May 2021).

[31] R. Chen, K. Zhong, Z. Li, M. Liu, G. Zhan, An accurate and reliable circular coded target detection algorithm for vision measurement, in: S. Han, T. Yoshizawa, S. Zhang (Eds.), Proc. Opt. Metrol. Insp. ind. Appl. IV, SPIE, Beijing, China, 2016, pp. 1−10, https://doi.org/10.1117/12.2245590.